

An experimental study on ferromagnetic nickel nanowires functionalized with antibodies for cell separation

Ning Gao¹, Hongjun Wang² and Eui-Hyeok Yang^{1,3}

¹ Department of Mechanical Engineering, Stevens Institute of Technology, Castle Point on the Hudson, Hoboken, NJ 07030, USA

² Department of Chemistry, Chemical Biology and Biomedical Engineering, Stevens Institute of Technology, Castle Point on the Hudson, Hoboken, NJ 07030, USA

E-mail: eyang@stevens.edu

Received 17 October 2009, in final form 3 January 2010

Published 16 February 2010

Online at stacks.iop.org/Nano/21/105107

Abstract

In this paper, a cell separation technique has been explored using antibody-functionalized Ni nanowires. An antibody (anti-CD31) against mouse endothelial cells (MS1) was conjugated to the Ni nanowire surface through self-assembled monolayers (SAMs) and chemical covalent reactions. The measured cytotoxicity was negligible on the CD-31 antibody-functionalized nanowires by the tetrazolium salt (MTT) assay. The use of functionalized nanowires for magnetically separating MS1 cells revealed that the cell separation yield was closely related to cell concentration and the nanowire/cell ratio. Cell separation yield using functionalized Ni nanowires was compared with that using commercial magnetic beads. Considering the volume difference of the material used between the beads and nanowires, antibody-functionalized nanowires showed an obvious advantage in cell separation. Further study on the effect of Ni nanowires on MS1 cells for extended culture confirmed that cell morphology remained comparable to control cells with a lower proliferation rate. This work demonstrates that antibody-functionalized Ni nanowires provide an effective means to separate target cells.

1. Introduction

Cell separation is essential for many cell-based applications in biochemistry, immunology, cell and molecular biology, and clinical research. In clinical applications, cell purification is required to obtain a specific population for transplantation and gene therapy, or to isolate the stem and progenitor cells for cancer treatment [1, 2]. While a range of cell separation techniques have been developed [3], super-paramagnetic iron oxide beads (e.g. Fe₃O₄) coated with antibodies specific for the surface antigens of target cells have been widely used [4, 5]. During cell separation, the target cells from a mixed cell population are attached to the magnetic beads via antibody-antigen interactions and then separated by an external magnetic field. However, high external gradient magnetic fields are typically required in order to efficiently fractionate the cells, especially in continuous flow cell separation. A high-gradient

magnetic concentrator (HGMC) with a high magnetic field has been used to capture cells rapidly from a continuous flow to achieve high-speed separation [6–9]. Recently, ferromagnetic nickel (Ni) nanowires have been introduced in magnetic cell manipulation [10–18] to utilize their high aspect ratio, shape anisotropic properties, and high residual (M_R) and intrinsic magnetization (M_S). Studies have shown that ferromagnetic Ni nanowires outperform super-paramagnetic magnetic beads in cell separation, since the saturation magnetization of Ni nanowires is over an order-of-magnitude higher than that of the magnetic beads [10, 14]. The distinctive peculiarities of nanowires potentially enable applications in controlling the spatial organization of cells [15], transporting cells [16], applying force to living cells [17], inducing hyperthermia in cells [18] and improving separation speed in continuous flow.

While the fabrication of Ni nanowires using an electrodeposition technique [19, 20] has been widely studied, the chemical modification of Ni nanowire surfaces is not fully explored, especially in the case of antibody functionalization.

³ Author to whom any correspondence should be addressed.

In previous studies, Ni nanowires exhibited a tendency of being internalized by cells [10, 14, 15, 21]. This cell–nanowire interaction is governed solely by the affinity of the cells and hydrophilic surfaces; therefore the target cells cannot be separated selectively from the mixed cells. Moreover, Ni nanowires were incubated with cells for 24 h to improve the nanowire internalization [10], significantly limiting their applicability in cell separation. Therefore, a considerable modification is necessary for the desired and specific bioactivity. Our preliminary results showed that functionalized Ni nanowires could effectively separate nanowire-bound target cells from the mixture of cells. In this paper, efforts have been made to further study the functionalization of Ni nanowires with antibodies and comparison of the separation efficiency of target cells with antibody-functionalized nanowires and antibody-functionalized super-paramagnetic iron oxide beads. Additionally, the cytotoxicity of Ni nanowires and their effect on cell proliferation have been studied and compared with iron oxide beads.

2. Experimental methods

2.1. Materials

The alumina nanotemplates were obtained from Anodisc 25 Waterman Inc. (Maidstone, UK). Gold plating solution, Orotemp 24 TRU, was obtained from Technic Inc. (Cranston, RI). Gold etchant TFAC was supplied by Transene (Danvers, MA). 1-ethyl-3-[3-dimethylaminopropyl] carbodiimide hydrochloride (EDC) and *N*-hydroxysulfosuccinimide (sulfo-NHS) were purchased from Pierce Biotechnology, Inc. (Rockford, IL). Pimelic acids, streptavidin, BSA, NaN_3 , thiazolyl blue tetrazolium bromide (MTT) and dimethyl sulfoxide (DMSO) were obtained from Sigma (St Louis, MO). Biotin anti-CD31 was supplied by eBioscience (San Diego, CA). Mouse endothelial cells (MS1 CRL-2279), Dulbecco's Modified Eagle's Medium (DMEM) and fetal bovine serum (FBS) were purchased from American Type Culture Collection (ATCC, Manassas, VA). Epoxy-coated M-450 magnetic beads (14011), rat anti-mouse CD31 (RM5200) and all the other reagents and solutions were obtained from Invitrogen (Carlsbad, CA), except where indicated.

2.2. Biofunctionalization of Ni nanowires

Ni nanowires (25 μm long) were fabricated by electrodeposition using alumina nanotemplates with 200 nm parallel pores [16]. Ni nanowires were functionalized with CD-31 antibodies following the sequence shown in figure 1. Briefly, Ni nanowires were incubated with 2 mM pimelic acid/ethanol solution in a 1.5 ml microcentrifuge tube for 24 h. They were then washed sequentially with ethanol five times, 70% ethanol twice and PBS twice. EDC and sulfo-NHS solutions were freshly made in cold PBS before use. A mixture of 160 μl of EDC solution, 160 μl of sulfo-NHS solution and 80 μl streptavidin were added to the washed nanowires at the final concentrations of 2 mM EDC, 5 mM sulfo-NHS and 100 μM streptavidin, and incubated for 3 h at room temperature with slow tilting rotation. After incubation, the tube was placed on a magnet for 3 min

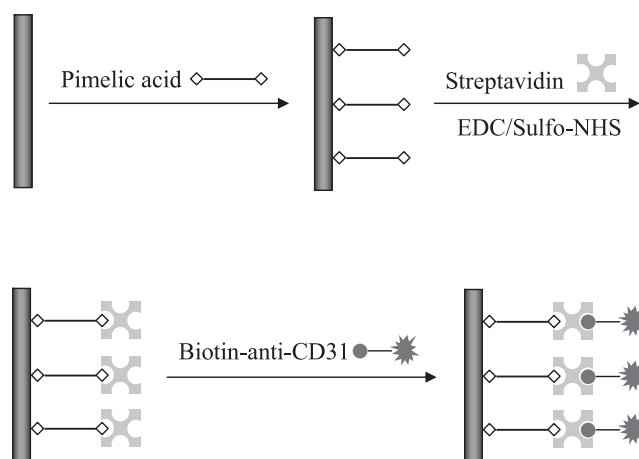


Figure 1. Illustration of the functionalization of Ni nanowires with CD31 antibodies. First, nanowires are incubated with the pimelic acid linker and form carboxyl group ends through carboxyl group self-assembled monolayers (SAMs). Then, amine groups of streptavidins are linked to carboxyl groups by EDC and sulfo-NHS. Finally, the antibody CD31 is bound onto the surface of the nickel nanowires by streptavidin–biotin coupling.

and the supernatant was discarded. Nanowires were washed with PBS seven times to remove any excess reagent under the magnetic field. The streptavidin-coated nanowires were re-suspended by sonicating for 10 min to obtain well-dispersed nanowires before antibody functionalization. The nanowires and 50 μg biotin anti-CD31 were then incubated in 400 μl PBS for 30 min under gentle rotation. To remove excess antibodies, the coated nanowires were washed seven times with PBS. The final antibody-coated nanowires were re-suspended in PBS and stored at 4 °C for future use. Functionalized nanowires were counted by erythrocytometry and diluted to the desired concentration prior to use.

2.3. Biofunctionalization of iron oxide beads

The 4.5 μm -diameter epoxy coated M-450 magnetic beads (300 μl) were washed twice and re-suspended in 0.1 M sodium phosphate solution at pH of 7.6. Then, 40 μg rat anti-mouse CD31 (200 μl) was added to 200 μl bead solution. After 15 min of incubation at room temperature, 5% BSA was added with a final concentration of 0.1%, and the beads were incubated for 20 h at room temperature under gentle mixing with a rotator. The beads were then washed three times with 0.1% BSA/PBS (pH 7.4). Finally, anti-CD31-coated beads were stored in PBS with 0.1% BSA and 0.02% NaN_3 at 2–8 °C. The functionalized beads were similarly counted by erythrocytometry and diluted to the desired concentration prior to use.

2.4. Immunofluorescence staining of functionalized nanowires and beads

The rabbit anti-rat IgG secondary antibody labeled with Alex Fluor 594 (red fluorescence), at a final concentration of 10 $\mu\text{g ml}^{-1}$, was added to the antibody CD31-functionalized nanowires or beads in PBS. Each mixture was incubated for

1 h at room temperature under gentle rotation. Excessive antibodies were removed by intensive washing with PBS. The fluorescence-labeled nanowires and beads were examined under a Nikon 80i fluorescent microscope.

2.5. Cell culture process

Mouse endothelial cells (MS1), positive for CD31 antigen, were used in this study. MS1 cells were cultured in DMEM supplemented with 1% penicillin/streptomycin and 5% fetal bovine serum at 37 °C. Subculture was routinely performed at a 60–70% confluence using 0.25% trypsin-EDTA to detach the cells.

2.6. Cell viability measurement by tetrazolium salt (MTT) assay

To determine the cytotoxicity of Ni nanowires, MS1 cells (2.0×10^4 cells per well) were seeded into 12-well plates and cultured overnight. Then, fresh medium containing either 1.0×10^5 functionalized Ni nanowires or microbeads was added to the plates and cultured for another 24 h. The cells were then incubated with thiazolyl blue tetrazolium bromide solution (0.5 mg ml^{-1} in culture media) for 3 h at 37 °C in a dark CO₂ incubator. Dimethyl sulfoxide (1 ml) was added to each well to extract the formazan product. The extract ($100 \mu\text{l}$) was transferred to a 96-well plate and the absorbance was measured at 570 nm with a Synergy HT Multi-Detection Microplate Reader (BioTek Instruments, Winooski, VT).

To evaluate whether the cell proliferation was affected by direct contact with Ni nanowires, after magnetic separation the nanowire-bound cells were counted and directly plated onto 12-well plates. The same amount of bead-bound cells or non-treated control cells, 1.0×10^4 cells per well, was similarly seeded onto the 12-well plates. The cells were then cultured for up to three days. The MTT assay was performed on the cultured cells to determine their proliferation.

2.7. Internalization preparation and imaging

4.0×10^4 cells were seeded on Si wafers in 12-well plates. 2.0×10^5 nanowires were added to 12-well plates after 12 h culture. The cells were washed three times with PBS after 0.5, 1, 2 and 4 h incubation and then were fixed with 2.5% glutaraldehyde in PBS for 30 min. After three times washing with PBS, the samples were dehydrated in a series of gradient ethanol (50%, 70%, 80%, 90% and 95% for 15 min and 100% twice for 15 min). The Si wafers were sputter-coated with gold before SEM observation.

2.8. Cell separation

MS1 cells and functionalized nanowires (or beads) were added to a sterile 1.5 ml centrifuge tube and incubated for 30 min with gentle rotation. After incubation, the tube was placed under a magnetic field for 3 min. The supernatant was discarded. Nanowire-bound cells (or bead-bound cells) were then washed three times by re-suspending in culture media before magnetic separation. Finally, the

Table 1. Calculated surface area and volume for microbeads and nanowires.

	Microbeads	Nanowires
Surface area (m^2)	$2.03 \times 10^{-11}\pi$	$5.04 \times 10^{-12}\pi$
Volume (m^3)	$1.52 \times 10^{-17}\pi$	$2.50 \times 10^{-19}\pi$
Surface area/volume ratio ($\times 10^6$)	1.33	20.2

separated nanowire-bound (or bead-bound) cells were counted by erythrocytometry. The separation yields were calculated by dividing the number of nanowire-bound (or bead-bound) cells by the initial total number of cells.

2.9. Statistical analysis

All quantitative results were obtained from at least three samples. Each experiment was repeated separately at least three times. Data were expressed as the mean \pm standard deviation (SD). An unpaired *t*-test was used in the statistical analysis of experimental data. A value of $p < 0.05$ was considered to be statistically significant.

3. Results and discussion

3.1. Antibody-functionalized nanowires and beads

To immobilize CD31 antibodies onto ferromagnetic Ni nanowires, the streptavidin–biotin coupling system was employed in this study (figure 1). Several approaches can be utilized to conjugate the antibody onto nanowires (invitrogen's dynabeads). The well-established streptavidin–biotin interaction would provide a reliable immobilization of antibodies onto the nanowires despite their possible low immobilization rate as a result of the steric hindrance from large streptavidin molecules. To determine the successful immobilization of CD 31 antibodies onto the nanowires and beads, Alex 594-conjugated secondary antibody was used to specifically detect the nanowire- or bead-bound anti-CD31 antibody. As shown in figure 2, uniform red fluorescence was observed on each nanowire or bead, indicating the immobilization of CD31 antibodies onto the surfaces of nanowires and beads. Comparable fluorescence intensity was observed among individual nanowires or beads, suggesting that the antibody functionalization was an equal event. In fact, the amount of antibody immobilized onto the nanowires or beads is significantly determined by the surface area and surface chemistry. Compared to microbeads, the surface area to volume ratio for nanowires is significantly higher (table 1), which suggests that more antibodies would be immobilized onto nanowires if the same weight of material is used.

The aggregation of antibody-functionalized nanowires was compared with that of bare (non-functionalized) nanowires. The two nanowire groups of the same concentration were suspended in the cell culture medium for 10 min under ultrasonication, and transferred onto a glass slide surface for observation under an optical microscope. From this experiment, no obvious difference was observed between them.

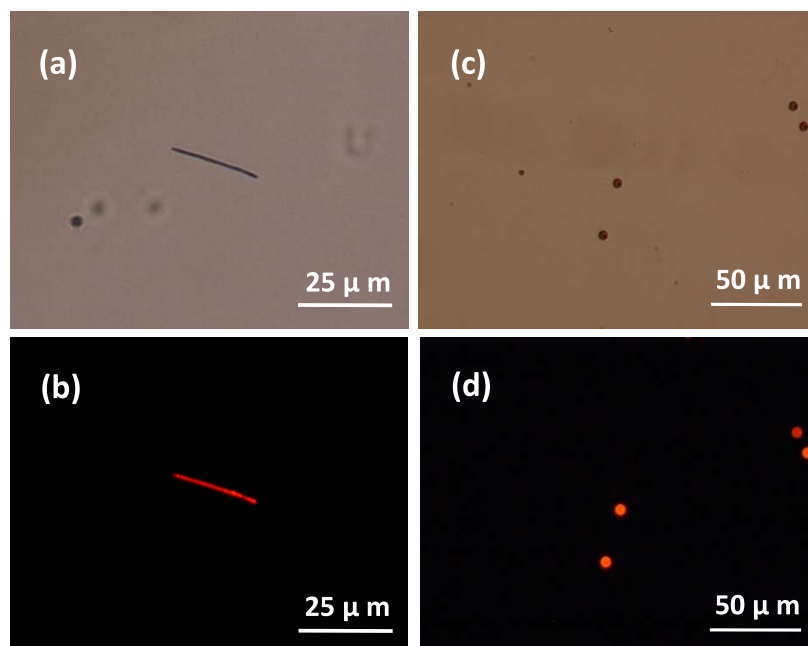


Figure 2. Images of nanowires and beads functionalized with CD31 antibody. Bright-field images of an Ni nanowire (a) and beads (c), and fluorescent images of a functionalized nanowire (b) and beads (d). The CD 31 antibody was detected by an Alex Fluor 594 (red) labeled secondary antibody.

(This figure is in colour only in the electronic version)

3.2. Cytotoxicity of functionalized nanowires

Cytotoxicity of Ni nanowires is critical in the cell separation technique described in this paper. To evaluate the cytotoxicity of Ni nanowires on the cells, an MTT assay was performed on the cells incubated with functionalized nanowires for 24 h. For comparison, functionalized magnetic beads were studied in tandem. Cells without any treatment were used as the control cells. The MTT results show that the cell viabilities with nanowires and beads are 90.0% and 87.3%, respectively (figure 3). No obvious toxicity was noticed for functionalized nanowires, which is consistent with the previous report that Ni nanowires were not toxic to the cells right after exposure [10]. However, cytotoxicity is greatly related to the nanowire/cell ratio. If the ratio is higher than 100, clear toxicity can be determined even after 10 h incubation [22]. In this study, the nanowire/cell ratio was kept down to 4–5 during cell separation to guarantee a low cytotoxicity.

3.3. Morphology and proliferation of the nanowire-bound cells

To determine the compliance of Ni nanowires to MS1 cells in a longer exposure period, two types of functionalized Ni nanowires ($1.0 \times 10^5 \text{ ml}^{-1}$) were prepared, i.e. highly dispersed and aggregated Ni nanowires. The mixture of both nanowires was mixed with $3.0 \times 10^5 \text{ ml}^{-1}$ MS1 cell suspension under gentle rotation at room temperature for 30 min. After magnetic separation, the nanowire-bound cells were seeded onto the tissue culture flask. The cell morphology cultured for 1 and 7 days respectively was observed under an inverted microscope (figure 4). The morphology of all the cells bound to both

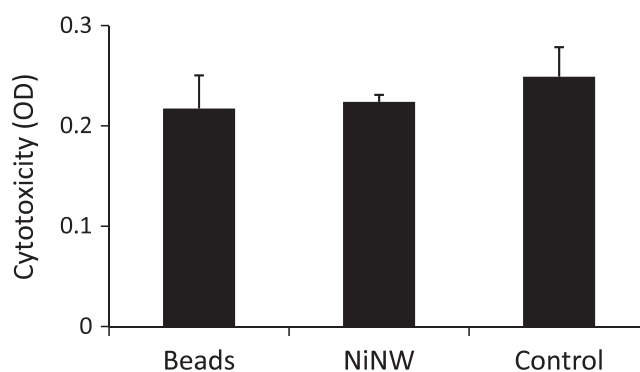


Figure 3. Cytotoxicity measurement of the functionalized beads and Ni nanowires (NW) using an MTT assay. MS1 cells (2.0×10^4 cells/well) were incubated with functionalized Ni NWs or beads at a concentration of $1.0 \times 10^5 \text{ ml}^{-1}$ for 24 h prior to the MTT assay.

the aggregated nanowires and the highly dispersed nanowires remained similar to those of the control group on day 1 (figure 4(a) versus (d)). The morphology of the cells bound to the highly dispersed nanowires is also similar to those of the control group on day 7 (figure 4(b) versus (e)). However, a noticeably lower number of cells were observed for the culture with aggregated nanowires than those of highly dispersed nanowires and controls after 7 days (figure 4(c) versus (e)). This result indicates that a locally high concentration of Ni nanowires due to aggregation is toxic to the cells. This observation is based on the qualitative assessment of the cell numbers between the nanowire-bound cells and the control cells, which is consistent with a previous report [22].

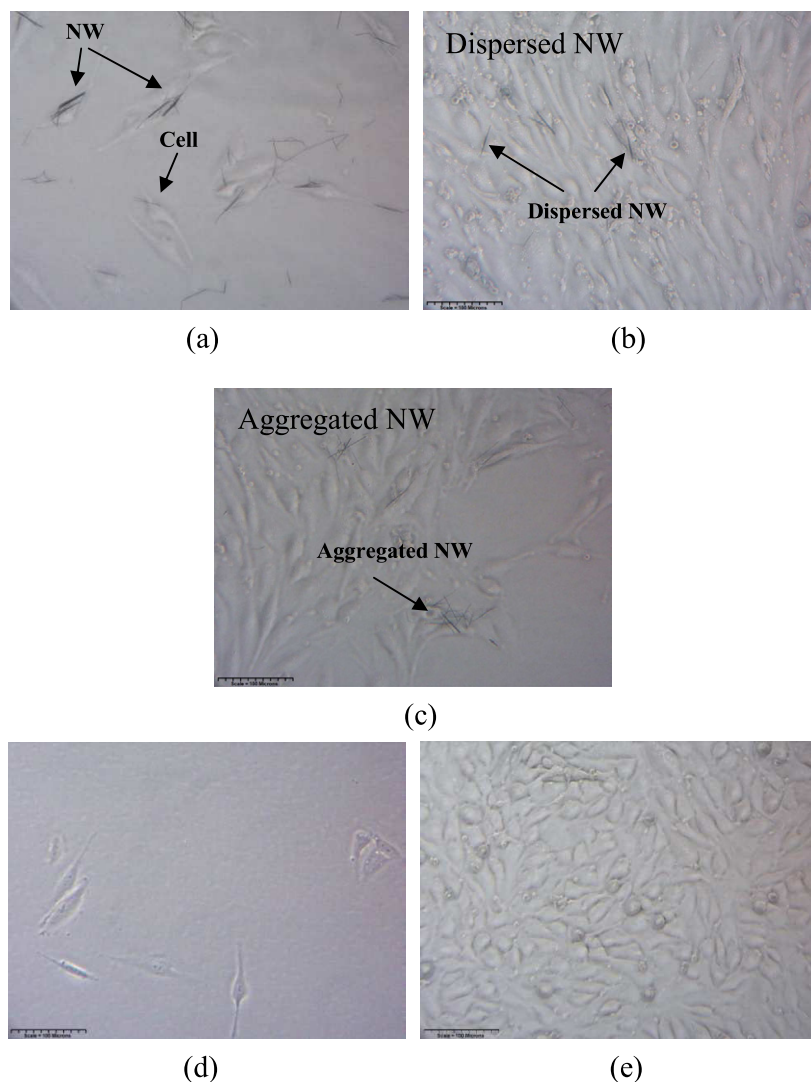


Figure 4. Images of nanowire (NW) bound cells ((a)–(c)) and control cells (d and e) cultured for 1 day ((a) and (d)) and 7 days ((b), (c) and (e)). The cell morphology remained similar between the culture with and without Ni nanowires. However, fewer cells were observed in the culture with higher NWs. Scale: 100 μm .

The effect of nanowires on cell proliferation was studied by culturing the magnetically separated nanowire-bound cells for prolonged periods (up to three days' post-cell separation). An MTT assay was performed to determine the cell metabolism and the results were summarized in figure 5. Clearly, a slower cell proliferation was observed for the nanowire-bound cells on the second and third days. However, the nanowire-bound cells continued to divide, with a similar doubling time (24 h) to the bead-bound cells and control cells. Taken together, these results indeed show that nanowires have some detrimental effects on the directly bound cell. This finding suggests that antibody-functionalized nanowires can be used to directly separate cells in a negative isolation or for a short-contact separation. In negative isolation, nanowire-bound cells (positive cells) are discarded, whereas intact cells (negative cells) are collected. However, in positive isolation, two possible approaches can be taken to avoid the toxicity of nanowires to the target cells by (1) detaching the cells from the nanowires right after cell separation, following the same

procedure as for the commercial cell separation bead product from Invitrogen or (2) discarding the nanowire-bound cells after cell proliferation. Additionally, nanowires can be coated with biocompatible polymer to reduce the toxicity for those applications with longer exposure [23]. However, in the case of cell separation, a polymer coating is not necessary for Ni nanowires for maintenance of the excellent magnetic properties of Ni nanowires.

3.4. Cellular internalization of nanowires

To compare the internalization of functionalized nanowires with that of non-functionalized bare nanowires, cells were incubated with nanowires for 0.5, 1, 2 and 4 h, respectively, and then observed using SEM. Approximately 40% MS1 cells bond to functionalized nanowires at 0.5 h while less than 4% cells bond to non-functionalized nanowires. The SEM results showed that nearly all the bonded functionalized nanowires attached to the outside of cell membranes. Nanowire

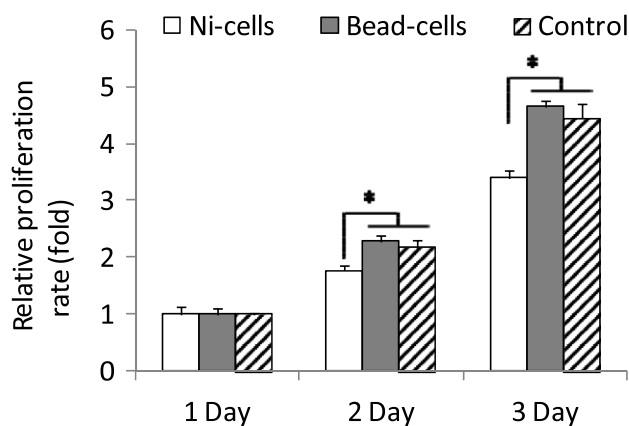


Figure 5. Proliferation of the nanowire-bound cells after cell separation. The cell proliferation was determined by MTT assay and relative rates to the first day reading were presented. * $p < 0.05$.

Table 2. The cell separation yields by different conditions.

Nanowire conc. ($\times 10^5$ wires ml^{-1})	Cell conc. ($\times 10^5$ cells ml^{-1})	Separated cells ($\times 10^5$ cells ml^{-1})	Separation yield (%)
4.0	1.0	0.43 ± 0.035	43 ± 3.5
4.0	4.0	1.3 ± 0.11	33 ± 2.8
4.0	16	3.1 ± 0.10	19 ± 0.62
10	5.0	1.9 ± 0.07	37 ± 1.4
20	5.0	3.0 ± 0.57	60 ± 11
40	5.0	2.7 ± 1.4	54 ± 2.8

internalization by cells started with the majority of bare nanowires ($\sim 70\%$ cell-bonded bare nanowires) after 1 h incubation (figure 6(a)). In contrast, most of the functionalized nanowires still attached to the outermost surfaces of the cells with tight binding to the cell membrane (figure 6(c)) even after 2 h incubation; the functionalized nanowires were rarely internalized by MS1 (arrow and asterisk in figure 6(b)). After 4 h, $\sim 50\%$ functionalized nanowires were internalized while $\sim 70\%$ bare nanowires were internalized. Yet, the degree of internalization of functionalized nanowires was considerably lower than that of bare nanowires (figure 6(d)). This variation is most likely due to the CD31 antibody conjugated onto the nanowires, which specifically interacts with the CD31 antigens located on the cell membranes.

3.5. Optimization of nanowire concentration for cell separation

We studied the effect of ‘cell concentration’ on the cell separation, while keeping the concentration of nanowires constant, $4.0 \times 10^5 \text{ ml}^{-1}$. The results are shown in table 2. The number of separated cells was increased as the cell concentration was increased, while the separation yield decreased. An increase in nanowire concentration can increase the binding opportunity of nanowires to cells, improving the separation yield; however, exorbitant concentrations can lead to nanowire aggregation, a common phenomenon for nanomaterials in suspension. The aggregation of nanowires will decrease cell separation efficiency and lead to cytotoxicity.

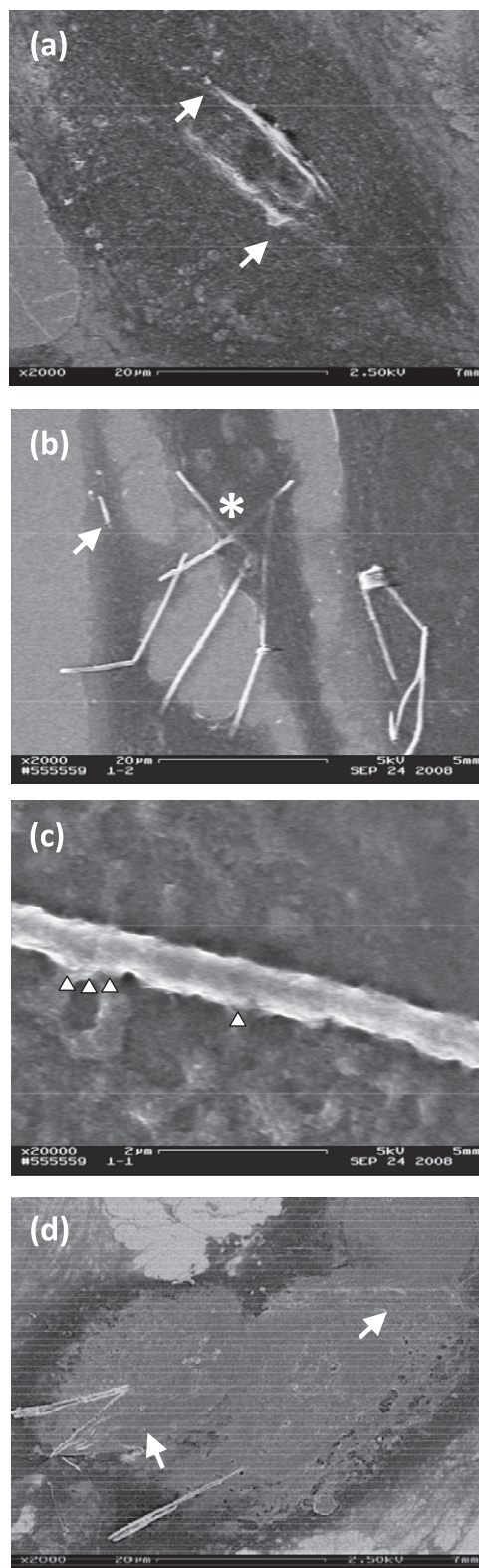


Figure 6. SEM images of the nanowire-bound cells cultured overnight after magnetic cell separation. After 1 h incubation, a bare nanowire inserted into cells (arrow) (a). After 2 h incubation, most of the functionalized Ni nanowires stayed on the surface of cell membrane, while a small amount of them were internalized either deeply inside the cells (arrow) or on the superficial region (asterisk) (b). After 2 h incubation, tight binding between Ni nanowires and cell membrane (arrowheads) was noticed for those nanowires attached to the cell surface (c). After 4 h incubation, a bare nanowire was completely internalized inside a cell (d).

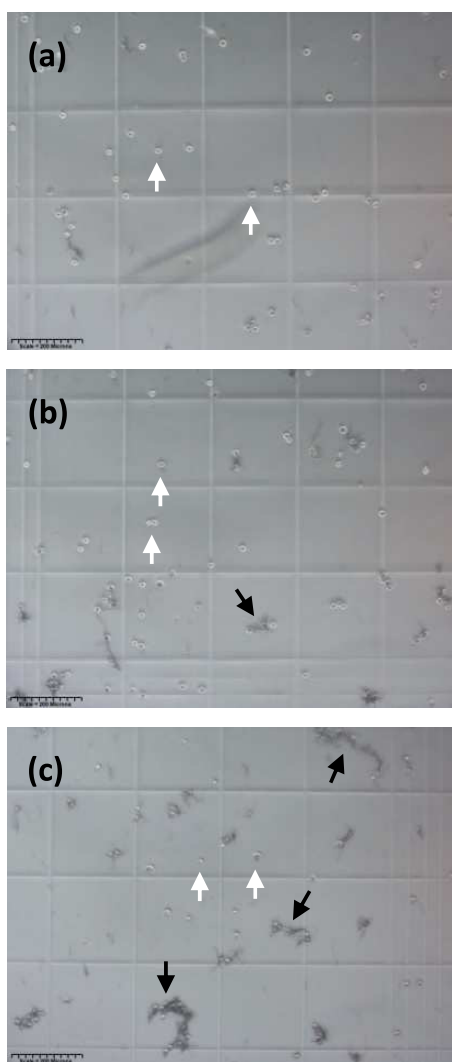


Figure 7. Images of the aggregated cell/nanowire (black arrows) among dispersed cells (white arrows) from erythrocytometry after magnetic separation. Nanowire concentrations (ml^{-1}): (a) 1.0×10^6 , (b) 2.0×10^6 and (c) 4.0×10^6 . Scale: $200 \mu\text{m}$.

To determine the appropriate nanowire concentration, 5.0×10^5 MS1 cells were mixed with different concentrations of nanowires. The separation yields at different ratios are summarized in table 2 and images of separated cells are shown in figure 7. Clearly, the cell separation yield increased with the increase in nanowire concentration and reached its peak separation yield at $2.0 \times 10^6 \text{ ml}^{-1}$. However, when the nanowire concentration increased to $4.0 \times 10^6 \text{ ml}^{-1}$, significant aggregation of nanowires was observed in the separated cell population (figure 7), resulting in a lower cell separation yield (table 2). In this regard, the optimal nanowire concentration for cell separation should be no more than $2.0 \times 10^6 \text{ ml}^{-1}$.

3.6. Comparison of separation yields of beads and nanowires

As magnetic beads are widely used for cell separation [2], it is necessary to compare cell separation efficiency between the functionalized Ni nanowires and the commercial magnetic beads under the same experimental conditions. Three different

Table 3. Comparison of the MS1 cell separation yields between beads and nanowires.

Cell conc. ($\times 10^5 \text{ cells ml}^{-1}$)		1.0	5.0	10
Microbeads	Conc. ($\times 10^5 \text{ beads ml}^{-1}$)	4.0	20	40
	Separation yield (%)	29 ± 3.5	60 ± 0.0	64 ± 6.7
Ni nanowires	Conc. ($\times 10^5 \text{ wires ml}^{-1}$)	4.0	20	40
	Separation yield (%)	43 ± 3.5	59 ± 7.0	63 ± 2.1

concentrations of MS1 cells, 1.0×10^5 , 5.0×10^5 and $1.0 \times 10^6 \text{ ml}^{-1}$, were used while maintaining the ratio of cell to bead or cell to nanowire at 1:4. The separation results showed that nanowires are either better or comparable to the beads for all three cell concentrations (table 3). At a lower cell concentration ($1.0 \times 10^5 \text{ cells ml}^{-1}$), the cell separation yield with nanowires was about 1.5 times that of the beads, while at high cell concentrations (5.0×10^5 and $1 \times 10^6 \text{ cells ml}^{-1}$) no clear difference was identified between nanowires and beads. A possible explanation is that long nanowires have a greater opportunity to interact with target cells than the beads at a lower concentration. However, at high concentrations, the aggregation of nanowires in the cell suspension (figure 7) would compromise their size advantage. This result also implies that the optimal condition for cell separation is to use a low concentration of cells and nanowires.

4. Conclusions

The use of antibody-functionalized ferromagnetic nanowires has been exploited for cell separation. In this study, the Ni nanowires functionalized with CD31 antibodies showed negligible cytotoxicity to MS1 cells. While the volume of nanowires used in the experiments is approximately 1/60 times lower than that of magnetic beads, the cell separation capacity of nanowires for MS1 was comparable to or better than that of magnetic beads. To achieve an optimal cell separation, the concentration of functionalized nanowires should be lower than $2.0 \times 10^6 \text{ ml}^{-1}$ to avoid nanowire aggregation. This work not only demonstrates that antibody-functionalized Ni nanowires are a promising alternative to microbeads for efficient cell separation, but also provides valuable data for the application of antibody-functionalized nanowires in cell separation.

Acknowledgments

The author would like to thank Xiaochuan Yang, Kitu Kumar and Yao-Tsan Tsai for their assistance in this experimental study.

References

- [1] Recktenwald D and Radbruch A 1997 *Cell Separation Methods and Applications* 1st edn (New York: Dekker)
- [2] Kumar A, Galaev I Y and Mattiasson B 2007 *Cell Separation* (Berlin: Springer)
- [3] Radisic M, Iyer R K and Murthy S K 2006 Micro- and nanotechnology in cell separation *Int. J. Nanomed.* **1** 3–14

- [4] Neurauter A A, Bonyhadi M, Lien E, Nøkleby L, Ruud E, Camacho S and Aarvak T 2007 Cell isolation and expansion using Dynabeads *Adv. Biochem. Eng. Biotechnol.* **106** 41–73
- [5] Pankhurst Q A, Connolly J, Jones S K and Dobson J 2003 Applications of magnetic nanoparticles in biomedicine *J. Phys. D: Appl. Phys.* **36** R167–81
- [6] Berger M, Castellino J, Huang R, Shah M and Austin R H 2001 Design of a microfabricated magnetic cell separator *Electrophoresis* **22** 3883–92
- [7] Chalmers J J, Zborowski M, Sun L and Moore L 1998 Flow through, immunomagnetic cell separation *Biotechnol. Prog.* **14** 141–8
- [8] Xia N, Hunt T P, Mayers B T, Alsberg E, Whitesides G M, Westervelt R M and Ingber D E 2006 Combined microfluidic-micromagnetic separation of living cells in continuous flow *Biomed. Microdev.* **8** 299–308
- [9] Adams J D, Kim U and Soh H T 2008 Multitarget magnetic activated cell sorter *Proc. Natl Acad. Sci. USA* **105** 18165–70
- [10] Hultgren A, Tanase M, Chen C S, Meyer G J and Reich D H 2003 Cell manipulation using magnetic nanowires *J. Appl. Phys.* **93** 7554–6
- [11] Hultgren A, Tanase M, Chen C S and Reich D H 2004 High-yield cell separations using magnetic nanowires *IEEE Trans. Magn.* **40** 2988–90
- [12] Reich D H, Tanase M, Hultgren A, Bauer L A, Chen C S and Meyer G J 2003 Biological applications of multifunctional magnetic nanowires *J. Appl. Phys.* **93** 7275–80
- [13] Bauer L A, Birenbaum N S and Meyer G J 2004 Biological applications of high aspect ratio nanoparticles *J. Mater. Chem.* **14** 517–26
- [14] Hultgren A, Tanase M, Felton E J, Bhadriraju K, Salem A K, Chen C S and Reich D H 2005 Optimization of yield in magnetic cell separations using nickel nanowires of different lengths *Biotechnol. Prog.* **21** 509–15
- [15] Tanase M, Felton E J, Gray D S, Hultgren A, Chen C S and Reich D H 2005 Assembly of multicellular constructs and microarrays of cells using magnetic nanowires *Lab on a Chip* **5** 598–605
- [16] Choi D, Fung A, Moon H, Ho D, Chen Y, Kan E, Rheem Y, Yoo B and Myung N 2007 Transport of living cells with magnetically assembled nanowires *Biomed. Microdev.* **9** 143–8
- [17] Sniadecki N J, Anguelouch A, Yang M T, Lamb C M, Liu Z, Kirschner S B, Liu Y, Reich D H and Chen C S 2007 Magnetic microposts as an approach to apply forces to living cells *Proc. Natl Acad. Sci. USA* **104** 14553–8
- [18] Choi D S *et al* 2008 Hyperthermia with magnetic nanowires for inactivating living cells *Nanosci. Nanotechnol.* **8** 2323–7
- [19] Chauré N B, Stamenov P, Rhen F M F and Coey J M D 2005 Oriented cobalt nanowires prepared by electrodeposition in a porous membrane *J. Magn. Mater.* **290** 1210–3
- [20] Chiriac H, Moga A E, Urse M and Óvári T A 2003 Preparation and magnetic properties of electrodeposited magnetic nanowires *Sensors Actuators A* **106** 348–51
- [21] Prina-Mello A, Diao Z and Coey J M 2006 Internalization of ferromagnetic nanowires by different living cells *J. Nanobiotechnol.* **4** 9
- [22] Byrne F, Prina-Mello A, Whelan A, Mohamed B M, Davies A, Gun'ko Y K, Coey J M D and Volkov Y 2009 High content analysis of the biocompatibility of nickel nanowires *J. Magn. Mater.* **321** 1341–5
- [23] Magnin D, Callegari V, Mátéfi-Tempfli S, Mátéfi-Tempfli M, Glinel K, Jonas A M and Demoustier-Champagne S 2008 Functionalization of magnetic nanowires by charged biopolymers *Biomacromolecules* **9** 2517–22